



16th WCCM / 4th PANACM 2024 · MS 0304 · W241652

An improved multi-level hp finite cell method for efficient thermo-viscoplastic analyses

Oliver Wege^a · Jan Niklas Schmäke · Martin Ruess

^aoliver.wege@hs-duesseldorf.de

University of Applied Sciences Düsseldorf · Germany

Vancouver, CA · July 26, 2024

Finite cells with adaptive overlay refinements

Ingredients of the underlying method

The finite cell method

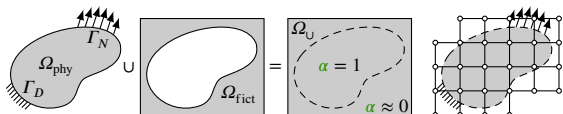


Figure: The fictitious domain approach to handle immersed boundaries.

- Immersed boundary method with high-order Ansatz spaces
- Modified weak form for e.g. the Poisson problem reads

$$\int_{\Omega_U} \alpha \nabla v \cdot \nabla u \, d\Omega = \int_{\Omega_U} \alpha v s \, d\Omega + \int_{\Gamma_N} v \bar{q} \, d\Gamma + \int_{\Gamma_D} v \bar{q} \, d\Gamma$$
$$\wedge \quad u = \bar{u} \quad \forall x \in \Gamma_D$$

- Indicator function $\alpha(x)$ $\begin{cases} = 1 & \forall x \in \Omega_{\text{phy}} \\ \approx 0 & \forall x \in \Omega_{\text{fict}} \end{cases}$

Multi-level hp refinements

- Local refinements by superposition with arbitrary hanging nodes

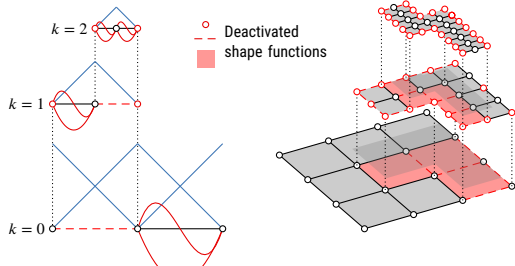


Figure: Multi-level hp scheme in 1D and 2D.

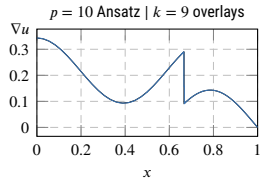
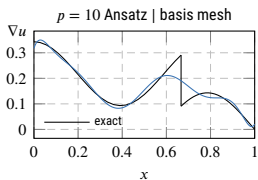


Figure: A 1D single element demonstration of a non-smooth problem.

Efficient integration of cut-cells

Non-negative moment fitting quadrature

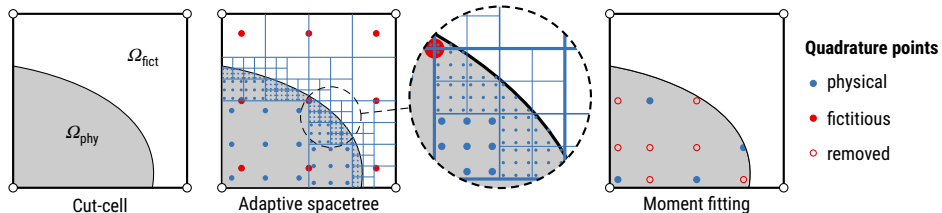


Figure: Numerical integration strategies for cut-cells.

Adaptive spacetree

- Recursively subdivide cut-cell into integration sub-cells
- Many quadrature points required for accurate integration
- Expensive recurring integration in nonlinear analyses

Non-negative moment fitting

- Moment fitting equations for m shape functions $N_j(\xi)$

$$\sum_{i=1}^n N_j(\xi_i) w_i = \int_{\Omega_{\text{phy}}} N_j(\xi) d\Omega \quad j = 1, \dots, m$$

- Initialization with n fixed points ξ_i and unknown weights w_i
- Solved with non-negative constrained weights $w_i \geq 0$ [Garhuom and Düster, 2022]
- Sparse set of points obtained using NNLS algorithm of [Lawson and Hanson, 1995]

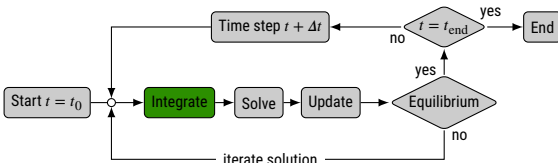
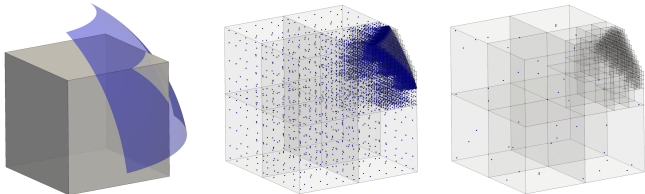


Figure: Elementary nonlinear solution scheme.

Efficient integration of cut-cells

Sphere-cut unit cell test



Number of quadrature points

- By a factor of ca. 1000 less points
- Reduction of 99.64% investing 6.5 times the effort

Accuracy

- Overall small error for $p = 1, \dots, 10$ integrands
- Increasing $p \rightarrow$ increasing integration error

Weakness

- Badly cut cells with small physical volume fraction

Indicator function
 $\alpha(\mathbf{x})$

Adaptive spacetree
(AST) **48250** points

Non-negative moment fitting
(NNMF) **175** points

Figure: Quadrature points in the sphere-cut unit cell with $p = 4$ basis.

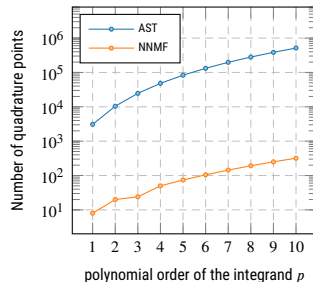


Figure: Number of points.

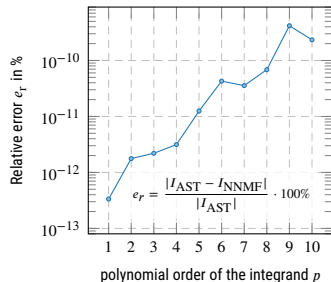


Figure: Integration error.

Thermo-viscoplasticity model

Rate-dependent J_2 flow theory with linear thermoelastic coupling

- Decomposition of strains in thermal, elastic and plastic

$$\boldsymbol{\epsilon} = \boldsymbol{\epsilon}^{\text{th}} + \boldsymbol{\epsilon}^{\text{e}} + \boldsymbol{\epsilon}^{\text{p}}$$

- Von Mises yield criterion

$$\Phi(\boldsymbol{\sigma}, \bar{\boldsymbol{\epsilon}}^{\text{p}}, T) = \sqrt{3J_2(\boldsymbol{\sigma})} - \sigma_y(\bar{\boldsymbol{\epsilon}}^{\text{p}}, T) \begin{cases} < 0 & \text{Elastic } (\dot{\gamma} = 0) \\ \geq 0 & \text{Plastic } (\dot{\gamma} \neq 0) \end{cases}$$

- Well-known viscoplastic constitutive relation [Perzyna, 1971]

$$\dot{\gamma}(\boldsymbol{\sigma}, \bar{\boldsymbol{\epsilon}}^{\text{p}}, T) = \begin{cases} \frac{1}{\mu(T)} \left[\frac{\sqrt{3J_2(\boldsymbol{\sigma})}}{\sigma_y(\bar{\boldsymbol{\epsilon}}^{\text{p}}, T)} - 1 \right]^{1/m(T)} & \text{if } \Phi \geq 0 \\ 0 & \text{if } \Phi < 0 \end{cases}$$

with relaxation time $\mu(T)$ and viscoplastic exponent $m(T)$

- Exponential isotropic strain hardening/softening
[Oppermann et al., 2022]

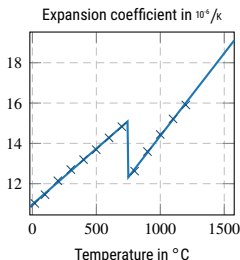
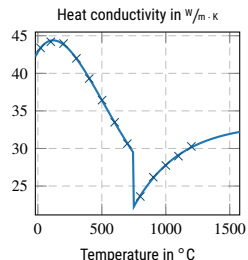
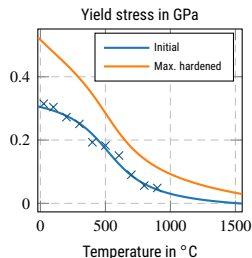
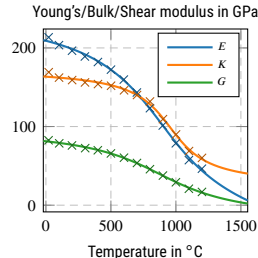
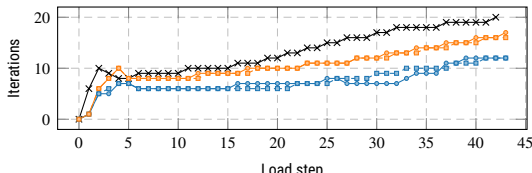
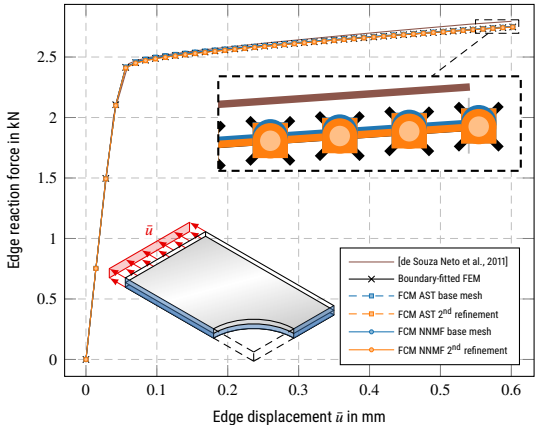


Figure: Material parameter interpolations for 16MnCr5 steel.

Isothermal method validation

Rate-independent comparison of the quadrature schemes



AST → Adaptive spacetree quadrature

NNMF → Non-negative moment fitting quadrature

Quality

- Load-displacement curves in good agreement
- Linear triangles of reference overestimate stiffness

Equilibrium convergence

- Roughly same for AST and NNMF
- Worsens slightly with increasing refinements

Efficiency

- NNMF requires 3 to 40 times the effort of AST to set up
- Still, ca. 30% reduction of total computation time

Cycle	AST	NNMF	Reduction
$i = 0$	20 412	2 468	87.91%
$i = 1$	38 031	6 039	84.12%
$i = 2$	58 544	14 389	75.42%

Table: Number of quadrature points.

Cycle	AST	NNMF	Reduction
$i = 0$	1.00	0.68	31.94%
$i = 1$	3.10	2.16	30.17%
$i = 2$	4.35	2.95	32.05%

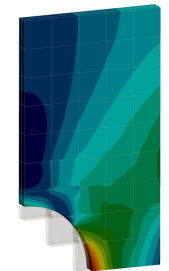
Table: Normalized computation effort.

Isothermal method validation

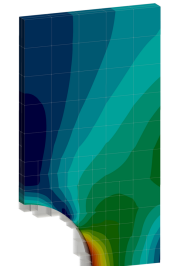
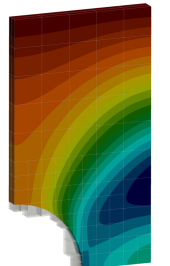
Viscoplastic analysis

- Von Mises plasticity model with isotropic linear strain hardening
- Perzyna-type viscoplasticity with $\mu = 500$ s and $m = 1$
- Deformation rate $\dot{\bar{u}} = 0.001$ & 0.01 mm/s

Ref. cycle Displacement magnitude $\|\bar{u}\|$ Accumulated plastic strain $\bar{\epsilon}^p$



$i = 0$



$i = 2$

Cycle	AST	NNMF	Reduction
$\dot{\bar{u}} = 0.001$ mm/s			
$i = 0$	20 412	2 468	87.91%
$i = 1$	41 730	6 928	83.40%
$i = 2$	59 300	17 148	71.08%
$\dot{\bar{u}} = 0.01$ mm/s			
$i = 0$	20 412	2 468	87.91%
$i = 1$	41 163	6 367	84.53%
$i = 2$	53 583	14 819	72.34%

Table: Number of quadrature points.

Cycle	AST	NNMF	Reduction
$\dot{\bar{u}} = 0.001$ mm/s			
$i = 0$	1.00	0.64	36.33%
$i = 1$	2.36	1.40	40.85%
$i = 2$	3.09	2.20	28.88%
$\dot{\bar{u}} = 0.01$ mm/s			
$i = 0$	1.00	0.69	31.50%
$i = 1$	2.25	1.49	33.70%
$i = 2$	2.79	2.05	26.43%

Table: Normalized computation effort.

Figure: Results of rate $\dot{\bar{u}} = 0.01$ mm/s with $m = 1.0$.

Numerical examples

Application to porous materials

Porosity defects

- Insufficient fusion in additive manufacturing of metals
- Trapped gas inclusions
- Voids due to thermal contraction when cooling

Consequences

- Reduction of resilience
- Increased risk for crack initiation
- Often not detectable by visual inspection

Analysis via FCM

- Non-destructive detection via computer tomography (CT)
- Straight-forward pipeline from CT-voxels to FCM mesh

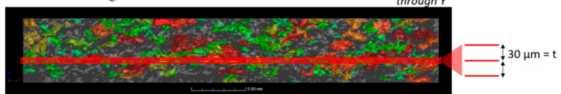
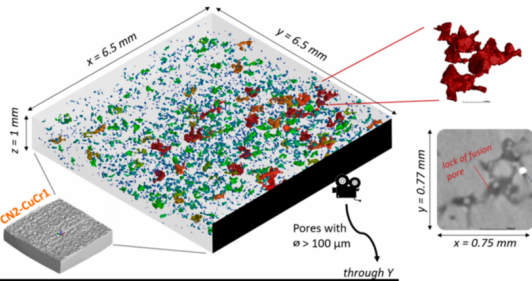


Figure: CT-scan of porosity in selective laser sintering (SLS).^a

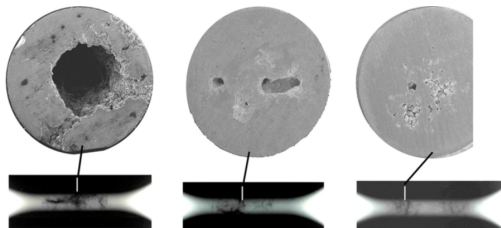


Figure: CT-scans of porosity in cast tensile specimen.^b

^a Sinico, M. et. al. (2021) in Materials, 14(8):1995.

^b Hardin, R.A. et. al. (2007) in Metallurgical and Materials Transactions A, 38(12):2992-3006.

Numerical examples

Thermo-viscoplastic plate model with porosity

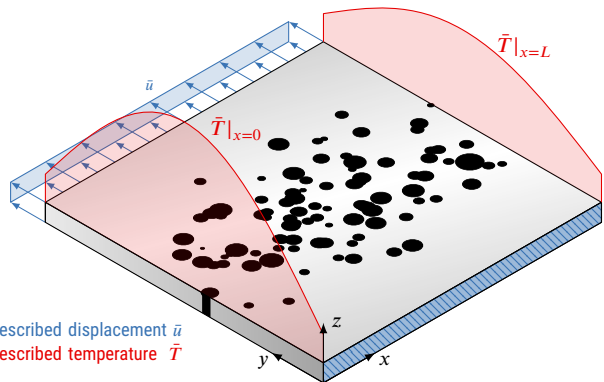


Figure: Thermo-mechanical problem setup.

- Base mesh of $10 \times 10 \times 1$ cells with $p = 2$ Ansatz
- Deformation rate $\dot{u} = 0.1 \text{ mm/s}$

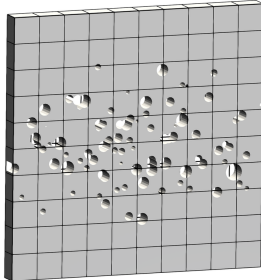


Figure: Base mesh.

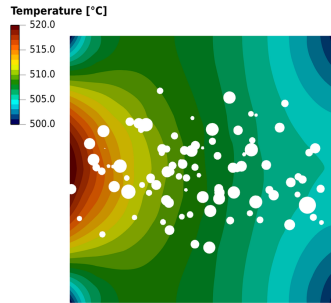
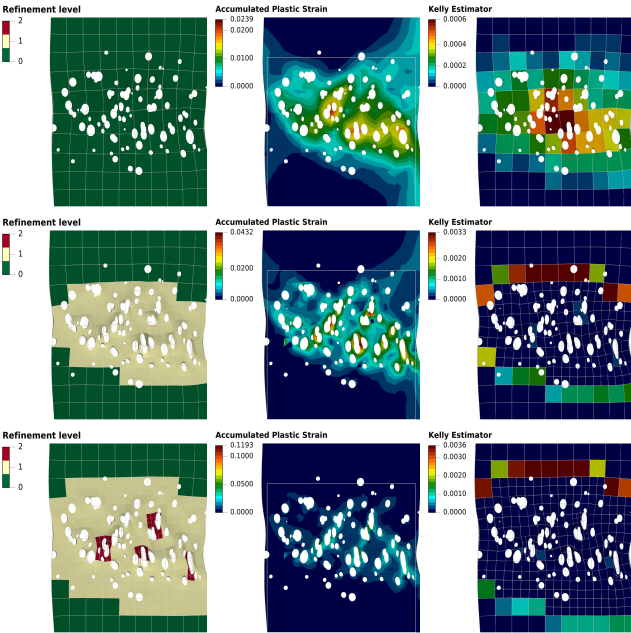
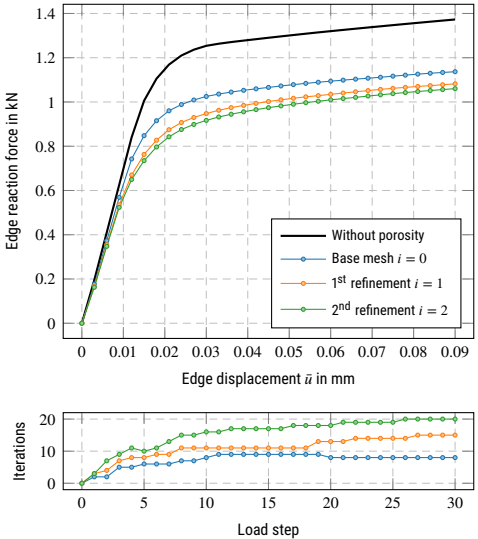


Figure: Temperature field at $t = 0 \text{ s}$.

Numerical examples

Thermo-viscoplastic plate model with porosity



Numerical examples

Thermo-viscoplastic plate model with porosity

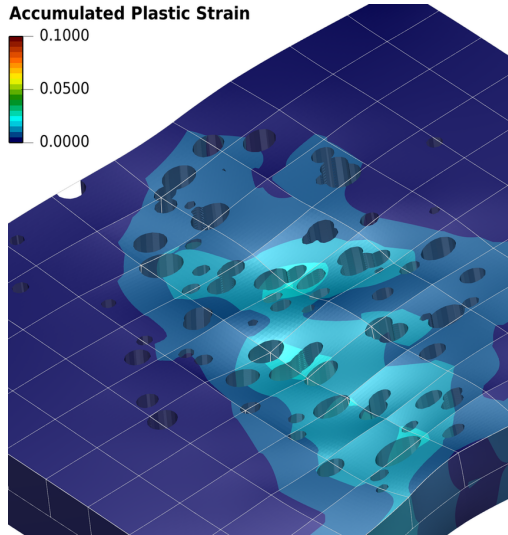


Figure: Base mesh (scaled by factor 30).

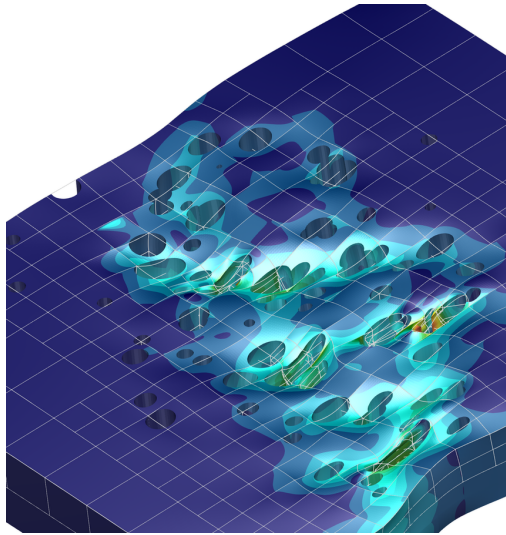
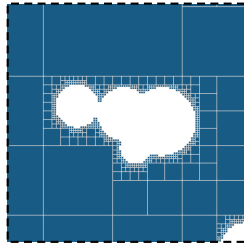


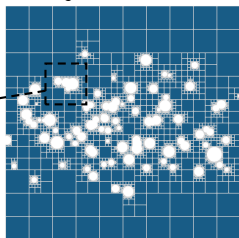
Figure: After 2nd refinement (scaled by factor 30).

Numerical examples

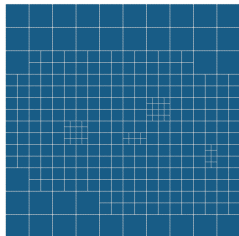
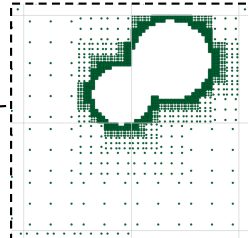
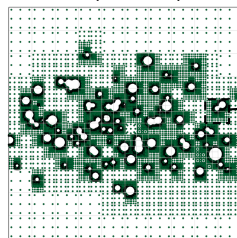
Thermo-viscoplastic plate model with porosity



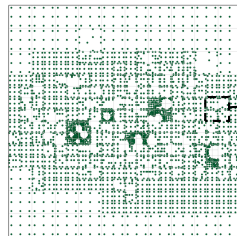
Adaptive spacetree
Integration on subcells



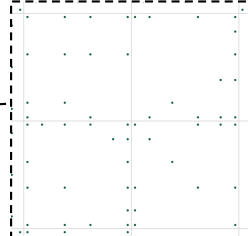
769 601 quadrature points



Integration on FE mesh
Non-negative moment fitting



30 295 quadrature points



Numerical examples

Thermo-viscoplastic plate model with porosity

- Reduction of quadrature points ca. 98%
- On average 95% runtime saved

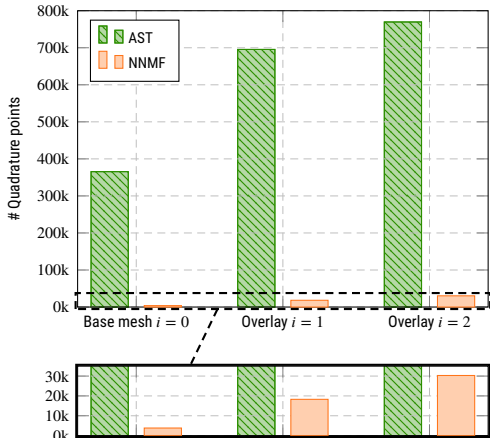


Figure: Number of quadrature points.

AST → Adaptive spacetree quadrature
NNMF → Non-negative moment fitting quadrature

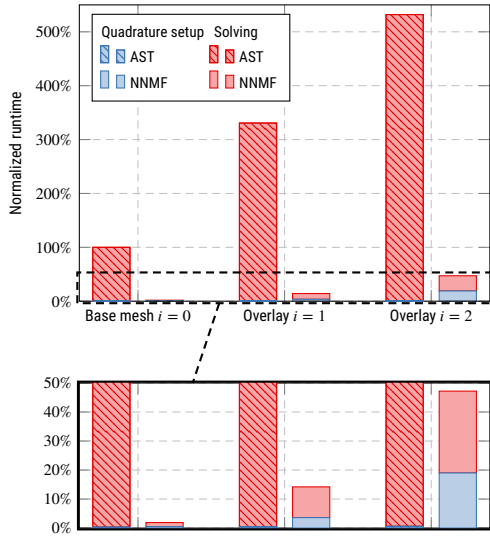


Figure: Computation runtime.

Numerical examples

CT-scan of a metal foam pore

- Geometry representation as gray-valued image slices
- Voxel-based indicator $\alpha(x)$ for inside-outside check

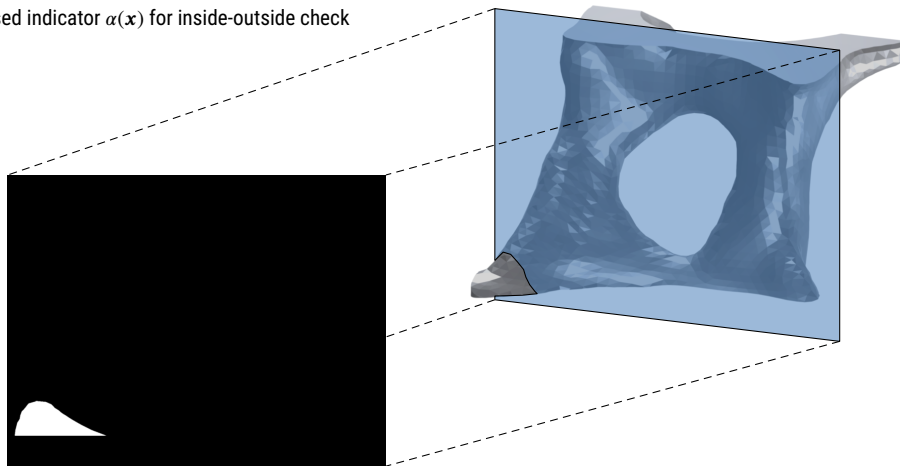


Figure: CT-scan voxel data as slices along the depth.

Numerical examples

CT-scan of a metal foam pore

- At temperature 20°C and 100°C
- Number of quadrature points

Adaptive spacetree	8 860 050
Non-negative moment fitting	131 715
Reduction	98.51%

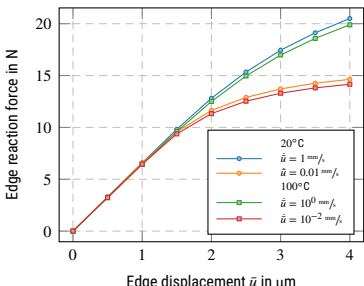


Figure: Load-displacement curves

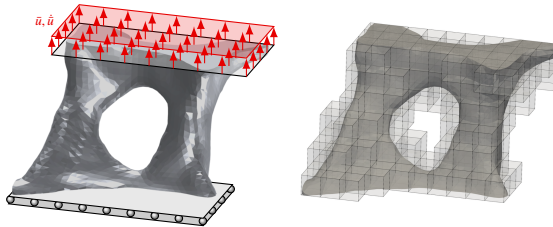


Figure: The metal foam pore model and finite cell base mesh.

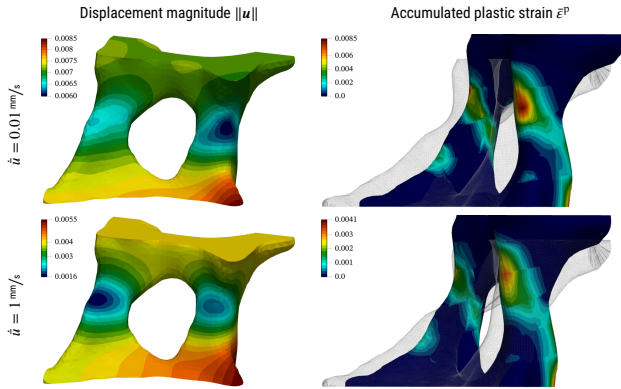


Figure: Results at 100°C.

An improved multi-level hp finite cell method for efficient thermo-viscoplastic analyses

Conclusion

- Reduction of quadrature points in cut-cells
 - 75% to 90% for simple benchmark
 - up to 98% for more complex geometries
- Significant reduction of computation effort
 - 30% for simple benchmark
 - 95% for more complex geometries – even for only 30 load steps
- Efficient method to analyze thermo-viscoplastic phenomena in complex structures
- Multi-level hp refinements improved quality of the plastic response

Outlook

- Bi-directional thermo-viscoplastic coupling with hyperplasticity
- Viscoplastic refinement metrics and anisotropic refinements
- Experimental creep test validation of porous metal samples



An improved multi-level hp finite cell method for efficient thermo-viscoplastic analyses

Oliver Wege

oliver.wege@hs-duesseldorf.de

Jan Niklas Schmäke

jan.schmaeke@hs-duesseldorf.de

Martin Ruess

martin.ruess@hs-duesseldorf.de

University of Applied Sciences Düsseldorf · Germany

Supported by the DFG project RU885/4-1

References

-  de Souza Neto, E. A., Perić, D., and Owen, D. R. J. (2011).
Computational methods for plasticity: theory and applications.
John Wiley & Sons.
-  Garhuom, W. and Düster, A. (2022).
Non-negative moment fitting quadrature for cut finite elements and cells undergoing large deformations.
Computational Mechanics, 70(5):1059–1081.
-  Lawson, C. L. and Hanson, R. J. (1995).
Solving least squares problems.
SIAM.
-  Oppermann, P., Denzer, R., and Menzel, A. (2022).
A thermo-viscoplasticity model for metals over wide temperature ranges-application to case hardening steel.
Computational Mechanics, 69(2):541–563.
-  Perzyna, P. (1971).
Thermodynamic theory of viscoplasticity.
Advances in applied mechanics, 11:313–354.